minerals

MDPI

Article

Influence of Sodium Hexametaphosphate on Muscovite Grinding and Its Mechanism Analysis

Chenyu Fan [1], Liuyi Ren [1,2,*], Yimin Zhang [1,2,3,4,*], Shenxu Bao [1,2] and Zhilu Yang [5]

[1] School of Resources and Environmental Engineering, Wuhan University of Technology, Wuhan 430070, China
[2] Hubei Key Laboratory of Mineral Resources Processing and Environment, Wuhan University of Technology, Wuhan 430070, China
[3] State Environmental Protection Key Laboratory of Mineral Metallurgical Resources Utilization and Pollution Control, Wuhan University of Science and Technology, Wuhan 430081, China
[4] Hubei Collaborative Innovation Center for High Efficient Utilization of Vanadium Resources, Wuhan University of Science and Technology, Wuhan 430081, China
[5] Xinjiang Nonferrous Metals Research Institute, Urumqi 830000, China
* Correspondence: rly1015@163.com (L.R.); zym126135@126.com (Y.Z.); Tel./Fax: +86-027-87651816 (L.R. & Y.Z.)

Abstract: In this paper, different doses of sodium hexametaphosphate (SHMP) were added as grinding aids in the process of muscovite grinding, and the effect of SHMP on the grinding efficiency of muscovite was studied. The grinding experiment results show that the grinding efficiency increases significantly with the increase in SHMP dosage. The mechanism of SHMP improving the grinding efficiency of muscovite was analyzed by various test methods. Experimental results showed that when SHMP was used as a grinding aid, the ordered structure of muscovite crystals was destroyed, the surface of muscovite was roughened, and obvious cracks appeared. SHMP was physically adsorbed on the muscovite powder, which effectively improved the pulp environment of muscovite powder during grinding, resulting in more dispersed muscovite powder, and improved the grinding efficiency. This study provides theoretical guidance for the efficient preparation of fine-grained muscovite powder and the action mechanism of grinding aids.

Keywords: grinding aids; muscovite; sodium hexametaphosphate; pulp dispersibility

check for updates

Citation: Fan, C.; Ren, L.; Zhang, Y.; Bao, S.; Yang, Z. Influence of Sodium Hexametaphosphate on Muscovite Grinding and Its Mechanism Analysis. *Minerals* **2023**, *13*, 457. https://doi.org/10.3390/min13040457

Academic Editors: Tsakalakis G. Konstantinos and Georgios Kolliopoulos

Received: 15 February 2023
Revised: 21 March 2023
Accepted: 22 March 2023
Published: 23 March 2023

Copyright: © 2023 by the authors. Licensee MDPI, Basel, Switzerland. This article is an open access article distributed under the terms and conditions of the Creative Commons Attribution (CC BY) license (https://creativecommons.org/licenses/by/4.0/).

1. Introduction

Muscovite is a hydroaluminosilicate mineral with a layered structure that can be formed under different geological conditions and is the most widely distributed mineral in the mica group [1]. Muscovite has good electrical insulation, heat insulation, high temperature resistance, acid and alkali corrosion resistance, luster, and stable physical and chemical properties [2,3]. Currently, muscovite powder with a particle size of D_{90} of about 45 μm is widely used in papermaking, latex paint, rubber, and other industries [4,5]. With the continuous development of the muscovite deep processing industry, high-grade coatings, pearlite, and other products have put forward higher requirements of muscovite powder. For example, pigments made from muscovite powder with a particle size of less than 20 μm have a satin sheen and are used to make a variety of inks. Muscovite powders with a particle size of 20 to 50 μm produce a pearly sheen and are commonly used to make clear or translucent plastic resins. Therefore, the preparation of fine-grained muscovite powder is an urgent problem to be solved [6,7].

Grinding is known as the most effective way to reduce particle size, but the energy consumption of the grinding process is high, so improving the grinding efficiency is an essential direction of grinding technology research [8]. Generally, grinding efficiency can be effectively improved by enhancing the capabilities of current grinding equipment or designing new equipment. Another approach is to improve the susceptibility of the material

to the grinding process [9,10]. During the grinding process of muscovite, the newly exposed surface of the flaky muscovite can be tightly combined along the cleavage plane. With the continuous reduction in the muscovite particle size, the defects of the particles decrease, the surface energy increases, the tendency of fine particles to agglomerate with each other is significantly enhanced, and the grinding efficiency decreases [11]. In order to obtain fine-grained muscovite products, wet stirring media grinding is usually used to reduce the particle size of muscovite. However, the effect of pure impact pulverization on the fine grinding of muscovite is poor, and the introduction of grinding aids has presented a suitable alternative. Today, grinding aids are widely used in the cement and ceramics industries [12–14]. The main goal of using grinding aids is to reduce grinding-specific energy consumption to obtain higher quality products or increase production capacity with the same energy consumption [15], and even reduce the influence of grinding operations on the environment, such as reducing carbon dioxide emissions caused by grinding [16].

The research on grinding aids has mainly focused on its grinding effect. Jinlin Yang et al. [17] compared the effects of sodium hexametaphosphate (SHMP), trethanolamine, ferric sulfate, aluminum chloride, polyaluminum chloride, and polyacrylamide on the particle size distribution of grinding products in order to reduce the overgrinding of cassiterite. The study found that the six grinding aids changed the particle size distribution of grinding products to varying degrees. The addition of polyacrylamide shortened the grinding time and increased the production of qualified particles. Yanru Chen et al. [18] found that ethanol is a better grinding aid in black talc grinding, which increases the refining speed of particles and eliminates the caking phenomenon between fine particles. Yan He et al. [19] synthesized a molecular-modified polycarboxylic acid-based grinding aid, and evaluated the grinding property of fine cement through the setting time, fluidity, heat of hydration, mechanical properties, and microstructure. The grinding aid increased the fineness of the cement, contributed to the hydration degree of the cement, and improved mechanical properties. Austin David et al. [20] found that SHMP strongly interacted with alumina-doped TiO_2 and improved the grinding properties under acidic and alkaline conditions.

SHMP has been introduced into the grinding process of rutile, cassis, and other minerals due to its wide application field, safety, and stability compared with other grinding aids [21–25]. At present, there is a lack of research on SHMP as a muscovite grinding aid. Most of the relevant research focus on the effect of the addition of SHMP on the grinding effect, and there are few detailed elaborations on the grinding aid mechanism of SHMP. In this paper, the grinding aid mechanism of SHMP on muscovite was studied by X-ray diffraction (XRD), Fourier transforms infrared spectroscopy (FT-IR), scanning electron microscope (SEM), energy dispersive spectrometer (EDS), and Zeta potential. The study is expected to provide a basis for the efficient production of fine-grained muscovite powder.

2. Materials and Methods

2.1. Materials

2.1.1. Mineral Samples

The raw muscovite used in this research was taken from Henan Province, China. Samples finer than 1.2 mm were obtained after crushing. The particle size characteristic curve of the sample is shown in Figure 1. Empyrean X-ray diffraction (XRD) instrument produced by PANalytical B.V. in the city of Almelo, The Netherlands was used to test the 2 cm × 2 cm muscovite sheet, and the test results are shown in Figure 2. The chemical composition of muscovite was studied using the Zetium X-ray fluorescence (XRF) spectrometer produced by PANalytical B.V. in Almelo, The Netherlands. For sample preparation, muscovite was ground to less than 0.074 mm, then dried for 2 h and placed at room temperature for testing. The test results are shown in Table 1. Figure 2 illustrates that muscovite has good crystallinity. It can be seen from Table 1 that the contents of SiO_2, Al_2O_3, and K_2O in the samples were 43.614%, 35.900%, and 8.360%, respectively. The muscovite content in the sample exceeds 90%, which met the experimental requirements.

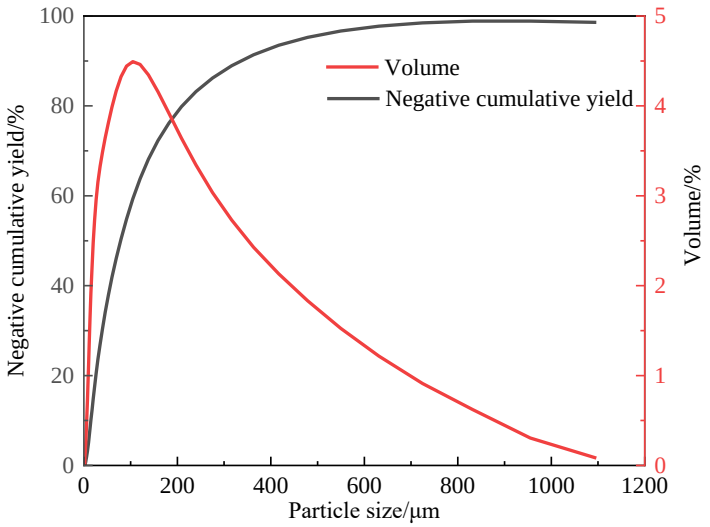


Figure 1. Characteristic curve of particle size of material.

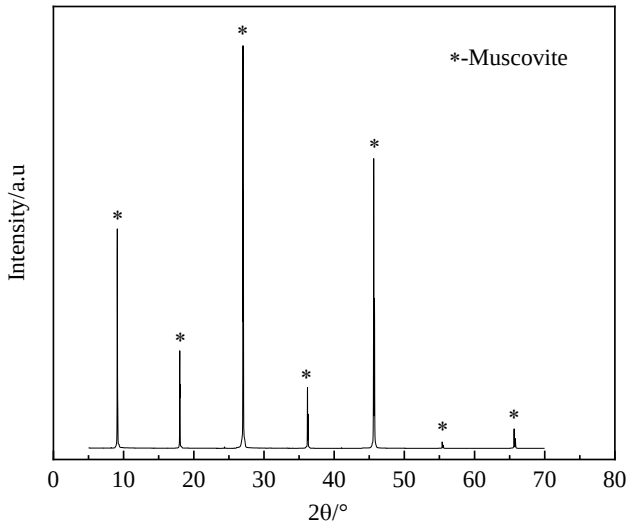


Figure 2. XRD of sample.

Table 1. XRF of sample.

Element	Content/%
SiO_2	43.614
Al_2O_3	35.900
K_2O	8.360
CO_2	4.904
Fe_2O_3	3.926
F	1.727
Na_2O	0.653
MgO	0.520
Rb_2O	0.396
MnO	0.163

2.1.2. Reagents

In this study, SHMP was the grinding aid for muscovite grinding. H_2SO_4 and NaOH were used to adjust the pH of the Zeta potential samples. All reagents used in this study were from Aladdin Reagents (Shanghai, China) and were analytical grade. The water used in the experiment and test is deionized water, and the conductivity is 18.25 MΩ.cm.

2.2. Methods

2.2.1. Muscovite Pure Mineral Grinding Test

The grinding experiments were performed using a JM-2A laboratory stirred ball mill produced by Tianchuang Powder Co., Ltd., Changsha City, Hunan Province, China. Through the preliminary exploratory experiments, the grinding conditions of muscovite were optimized. The grinding method used was wet grinding, and zirconia balls were used as the grinding media to minimize the contamination of the samples. The mill feed D_{90} = 361 μm and the particles above 100 μm accounted for 50%. The media filling rate was 50% (volume ratio); the grinding concentration was 40%; the speed of the mill was 400 r/min; the media size and mass ratio were m (Φ7 mm): m (Φ5 mm): m (Φ3 mm) = 1:4:1; the grinding time was 30 min. A total of 100 g of samples were put into each grinding, and then an appropriate dosage of grinding aid was dissolved in 150 g of water (the mass of grinding aid accounts for the percentage of the mass of muscovite). After grinding, the particle size of the ground product was analyzed using a BT-9300H laser particle size analyzer produced in Liaoning, China. The grinding experiment and particle size test were repeated five times. The grinding effect was evaluated by the content of −20 μm and −10 μm products.

2.2.2. XRD Analysis

An Empyrean X-ray diffractometer was used in this study to conduct an XRD analysis of the milled products. The high-voltage generator power of this instrument is 4 kW, the maximum high-voltage is 60 kV, the current and voltage stability is better than ±0.01%, and the 2θ angle measurement range is −10°~140°. In this study, XRD analysis was carried out on the grinding products under different dosages of SHMP to determine the effect of adding SHMP on the crystal structure of muscovite. The particle size of samples in this test was below 0.074 mm.

2.2.3. Vickers Hardness Analysis

HVS-1000 Vickers hardness tester was used to analyze the hardness changes in samples treated with different dosages of SHMP. The test force was 0.098 N, the magnification of the microscope was 400×, the magnification of the microscope was 100×, and the load retention time of the test force was 15 s. In this test, the same flake muscovite was cut into four pieces of 20 mm × 20 mm flake muscovite. Muscovite pieces were mixed in SHMP solution of different concentrations for 30 min, then dried and measured.

2.2.4. FT-IR Spectroscopy

The muscovite, SHMP, and samples after adding SHMP to aid grinding, were tested using a Nexus smart Fourier transform infrared spectrometer. The wavenumber range of this instrument used was 10,000–100 cm^{-1}, the highest resolution was 0.019 cm^{-1}, wavenumber accuracy was ±0.1 cm^{-1} and it was equipped with a brilliant single-point reflection accessory. Pure muscovite samples were ground to below 74 μm with a mortar before testing. The other mineral samples were grinding experiment products.

2.2.5. SEM and EDS Analysis

The JSM-IT300 scanning electron microscope produced in Japan was used to investigate the morphology of the muscovite raw materials and the grinding products treated with different dosages of SHMP. The instrument has a magnification of 5–300,000 times, a resolution of 3 nm in high vacuum mode, and an operating voltage of 15.0 kV. The Inca X-Act energy dispersive spectrometer produced in Germany was used for elemental analysis of the milled products with different dosages of SHMP. With a resolution better than 129 eV and an MK peak-to-back ratio of 20,000:1, the instrument can analyze elements 5B-92U. After washing and drying, the SEM and EDS tests were conducted on the grinding products. The powder was sprinkled on the double-sided tape on the sample table during sample preparation, and blow the powder in different directions with the rubber suction

bulb to ensure that the powder is firmly and evenly stuck on the double-sided tape. Gold spraying was performed prior to testing.

2.2.6. Pulp Dispersion Analysis

Two portions of 3 g muscovite powder and 100 mL deionized water were prepared to form a solution. One portion was added with 15 mg SHMP. Both were stirred in a magnetic agitator for 30 min and then precipitated for 2 h. The dispersion of muscovite powder was observed in two beakers.

The Nano-ZS90 Zeta Potentiometer was used to test the Zeta potential of muscovite powder after the action of different doses of SHMP in this study. During the test, the ambient temperature was kept at 25 °C, and the particle size of the sample was −5 μm. When the sample was prepared, the pulp was placed on a magnetic agitator to adjust the solution environment. After adjustment, the solution was stirred for 15 min to ensure that the pH would not change, so that the components in the pulp were fully mixed and reacted, and then allowed to stand for 5 min (settling was allowed). The supernatant of the settled solution was then removed with a disposable dropper and used to test for Zeta potential. In this test, the pH ranged from 3 to 11. Three samples of the same solution environment were prepared for each test, and the results were averaged for analysis.

3. Results and Discussion

3.1. Grinding Aid Effect of SHMP on Muscovite

In the grinding experiment, the dosage of SHMP was 0.2%, 0.5%, and 0.8%, respectively (percentage of SHMP and muscovite mass). The experimental results are shown in Figure 3.

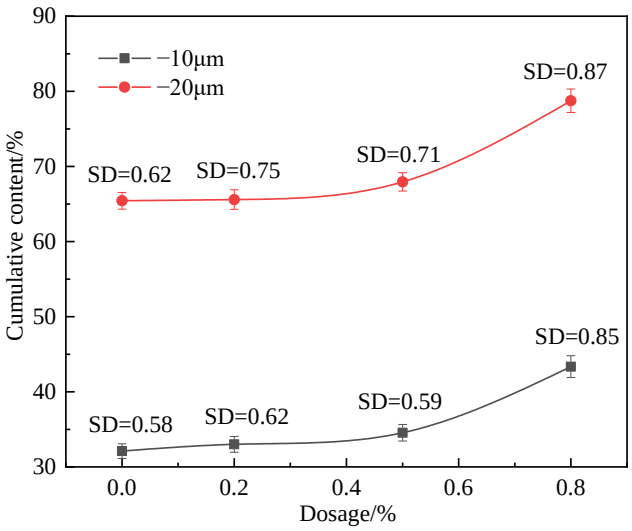


Figure 3. Grinding products −10 μm and −20 μm content.

It can be seen from Figure 3 that with the increase in the SHMP dosage, the content of −10 μm and −20 μm increased, and the standard deviation (SD) of each group of data are less than 1, which is representative. Without SHMP, the contents of −10 μm and −20 μm in muscovite products are 32.10% and 65.43%, respectively. When the dosage of SHMP is 0.8%, the contents of −10 μm and −20 μm in the muscovite products are 43.35% and 78.74%, which increased by 11.25% and 13.31%, respectively, compared with the products without SHMP.

The above data show that SHMP significantly affects the fine grinding of muscovite. This may be due to SHMP being absorbed on the surface of muscovite particles, which reduces the free energy of the surface of the particles, changes the particle hardness, and leads to the acceleration of the granularity of muscovite particles [26,27]. It is also possible that SHMP changes the pulp environment, improves the dispersion of muscovite particles

during the grinding process, reduces the pulp viscosity, and produces more fine-grained muscovite at the same grinding time [28,29]. This paper focuses on the grinding aid mechanism of SHMP on muscovite.

3.2. Effect of SHMP Dosage on Crystal Surface and Vickers Hardness of Muscovite

XRD analysis of muscovite grinding products with different SHMP dosages was carried out. The test results are shown in Figure 4.

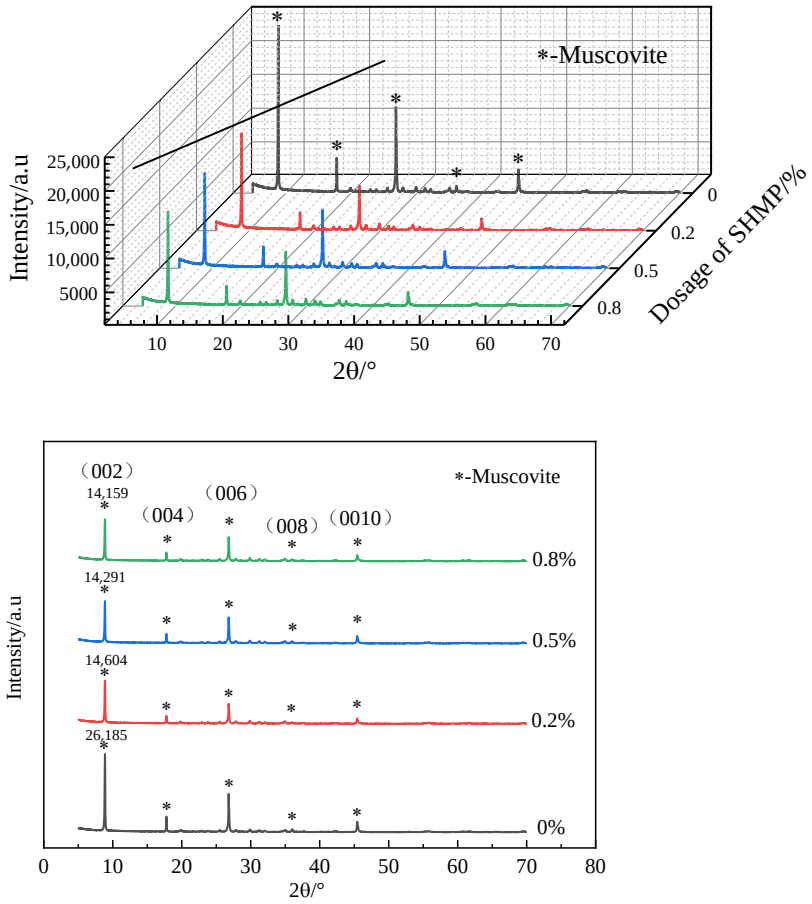


Figure 4. XRD analysis of muscovite products under different dosages of sodium hexametaphosphate (SHMP).

Figure 4 shows that the diffraction peak intensity of the principal crystal planes of the muscovite product is significantly reduced after the addition of SHMP. Compared with the XRD pattern of the muscovite product without SHMP, the primary diffraction peaks intensity of the muscovite product after adding SHMP is significantly reduced. Even the diffraction peak disappears or widens. The diffraction peak of the (002) plane decreases with the increase in SHMP dosage, and the diffraction peak of the (008) plane almost disappears. As the SHMP dosage increases, the particle size of muscovite products decreases, and the ordered crystal planes in muscovite decreases, resulting in the formation of amorphous muscovite lattice. The above data indicate that adding SHMP in the grinding process of muscovite makes the damage to muscovite more serious.

Reagent adsorption may change the hardness [30]. To determine the effect of SHMP on the muscovite hardness, the Vickers hardness test was conducted on muscovite treated with different dosages of SHMP. The test results are shown in Figure 5.

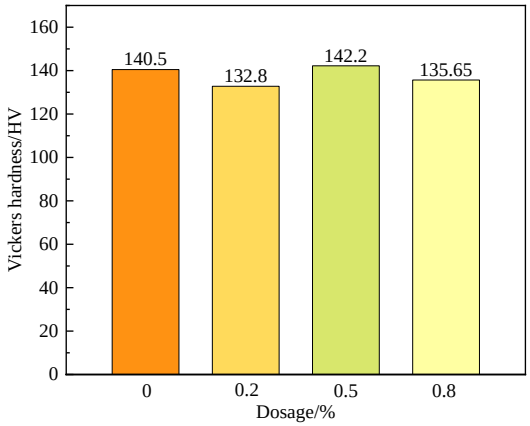


Figure 5. Effect of SHMP dosage on Vickers hardness of muscovite.

According to Figure 5, when the SHMP dosage is 0%, 0.2%, 0.5%, and 0.8%, the Vickers hardness of muscovite is 140.5 HV, 132.8 HV, 142.2 HV, and 135.65 HV respectively. With the increase in SHMP dosage, the Vickers hardness of muscovite do not change significantly after SHMP treatment. The serious damage of muscovite may be caused by the change of pulp properties.

3.3. Effect of SHMP Dosage on the Surface Functional Groups of Muscovite Grinding Products

To study the adsorption state of SHMP on the muscovite surface. FT-IR analysis was carried out on muscovite grinding products with different SHMP dosages. FT-IR test results are shown in Figure 6.

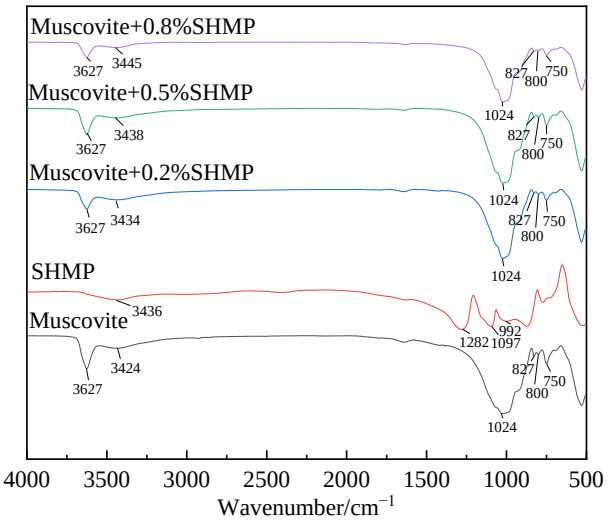


Figure 6. Infrared spectra of different samples.

In Figure 6, the absorption peaks of muscovite at 3627 cm^{-1} and 3424 cm^{-1} are the stretching vibrations of -OH in Al-O-H and Si-O-H groups. A total of 1024 cm^{-1} is the stretching vibration peak of Si-O group in muscovite, 800 cm^{-1} is the O-Si-O symmetric stretching peak, and 750 cm^{-1} is the symmetric stretching vibration peak of the Si-O [31,32]. In the spectrum of SHMP, 1282 cm^{-1} is the stretching vibration peak of P=O, and 1097 cm^{-1} and 992 cm^{-1} are the characteristic peaks of P-O [33]. With the increase in SHMP dosage, the absorption peak at 3424 cm^{-1} in the muscovite product spectrum shifted to 3445 cm^{-1}, indicating that -OH is affected by SHMP. However, there is no new absorption peak and the effective shift of other characteristic peaks in the infrared spectrum of muscovite with SHMP, indicating that SHMP may not chemically adsorbed on the muscovite surface. The reason for the shift in the absorption peak of -OH may be mechanical dehydroxylation [34].

3.4. Effect of SHMP Dosage on the Morphology and Surface Elements of Muscovite Grinding Products

In order to further illustrate that SHMP has a significant effect on muscovite grinding and the adsorption state of SHMP on the muscovite surface, SEM and EDS tests were carried out on muscovite raw materials and grinding products under different conditions. The results are shown in Figure 7.

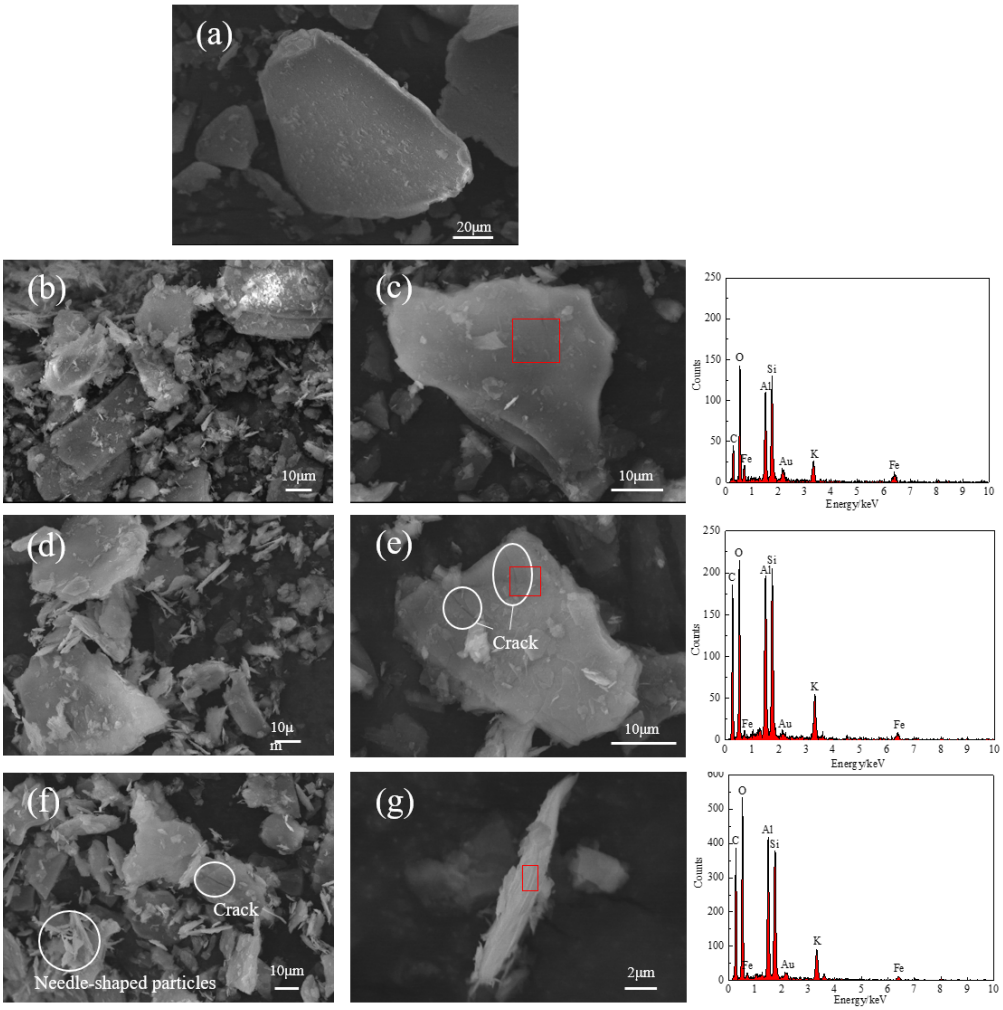


Figure 7. Surface morphologies of muscovite products with different dosages of SHMP (the red frame area is the EDS detection area). (**a**) Raw material, (**b**,**c**) no SHMP, (**d**,**e**) 0.2% SHMP, (**f**,**g**) 0.8% SHMP.

As shown in Figure 7a, the morphology of the muscovite powder without grinding showed an irregular flake shape, the surface is smooth and the boundary is clear. Figure 7b,d,f are the surface topography of muscovite products under a magnification of 1000 times. With the increase in the SHMP dosage, the needle-shaped muscovite particles decreased, the surface is roughened, the acicular muscovite fine particles increases, and the layered structure of muscovite is destroyed. There are apparent cracks perpendicular to the cleavage plane of muscovite in Figure 7f, the muscovite particles are obviously refined, and the effect of the SHMP grinding aid is significant. This conclusion is consistent with the results of XRD and grinding experiments. Figure 7c,e,g shows that the muscovite product with SHMP grinding has rough surfaces and cracks. The crack in grinding products may be due to the change in pulp environment with SHMP, which makes muscovite particles challenging to adhere to the media and increases the collision probability between particles and media. At the same grinding time, muscovite particles absorb more mechanical energy [31]. It can be seen from the regional EDS energy spectra of Figure 7c,e,g that there is

no peak of the P element in the muscovite products added with SHMP as a grinding aid. Because the sample was washed muscovite powder after grinding, it means that SHMP did not form firm chemical adsorption on the muscovite surface. However, it is due to the physical adsorption generated by van der Waals force. This conclusion is consistent with the results of FT-IR analysis.

3.5. Effect of SHMP on Dispersion of Muscovite Grinding Pulp

SHMP has a significant effect on the dispersibility of muscovite particles [35]. To intuitively understand the dispersion of SHMP, a settlement experiment was conducted. Two portions of 3 g muscovite powder and 100 mL deionized water were prepared to form a solution. One portion was added with 5% SHMP. Both were stirred in a magnetic agitator for 30 min and then precipitated for 2 h. The settlement results are shown in Figure 8.



Figure 8. Effect of SHMP on the dispersion of muscovite.

To further analyze the action mechanism of SHMP on muscovite grinding aid, the Zeta potential analyzer was used to measure the effect of different dosages of SHMP on the surface potential of muscovite. The test results of adding different dosages of SHMP to the surface potential of muscovite with the pH of the pulp are shown in Figure 9.

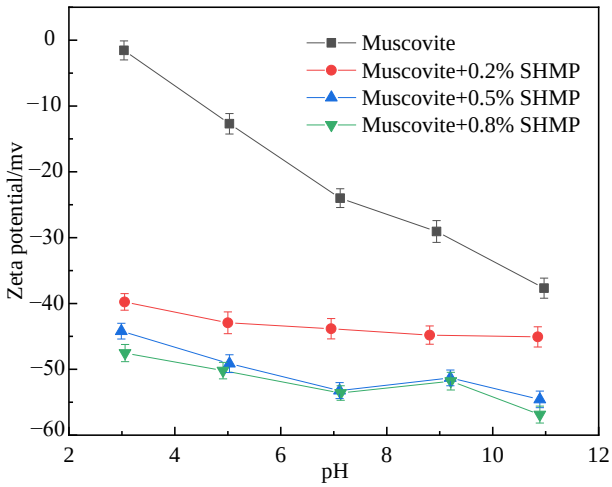


Figure 9. Influence of different dosages of SHMP on the surface potential of muscovite.

As shown in Figure 8, without SHMP, the solution is stratified after 2 h of settling, and fewer muscovite particles are dispersed. The sample with SHMP is turbid and the solution system is full of muscovite particles. From Figure 9, it can be seen that the action of SHMP on muscovite significantly reduces the pulp potential, increases the negative Zeta potential

of the muscovite surface, and increases the absolute value of the surface potential of the muscovite particles. Zeta potential shifted negatively with the increase in SHMP dosage. The pulp pH was measured between 7.3 and 8 in the grinding experiment.

In order to further explain the cause of Zeta potential change, the relationship between SHMP hydrolyzed components and pH was analyzed, and the results are shown in Figure 10. Figure 10 shows that when the pH value is between 7.3 and 8, SHMP in the pulp exists as HPO_4^{2-} and $H_2PO_4^-$ and attaches to the surface of the muscovite, which makes the Zeta potential of the muscovite surface increase negatively. Increasing the absolute value of Zeta potential on the surface of muscovite particles can enhance the mutual repulsion between muscovite particles and improve the dispersibility of the particles in the pulp [36,37]. The improved dispersion of muscovite particles prevents the fine particles from reuniting and adhering to the cylinder wall and increases the probability of collision between the particles and the grinding media, thus improving the grinding efficiency [38–40].

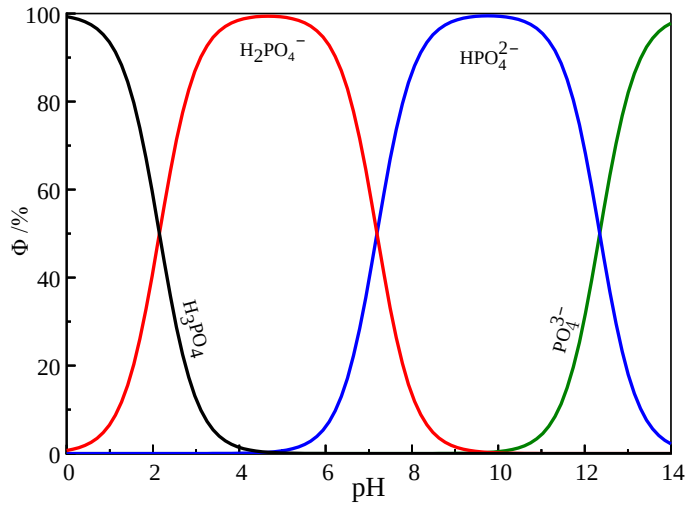


Figure 10. Distribution map of hydrolysis components of SHMP.

4. Conclusions

In the fine grinding process of muscovite, SHMP as a grinding aid can significantly improve the grinding efficiency of muscovite. When the dosage of SHMP was 0.8%, the −10 μm and −20 μm increased by 11.25% and 13.31%, respectively. When SHMP was added, the surface of the grinding product became rough, there were obvious cracks, needle-shaped particles increased, and the crystal order structure was destroyed more seriously. SHMP can significantly improve the dispersibility of pulp during the grinding of muscovite, mainly due to the physical adsorption of hydrolyzed HPO_4^{2-} and $H_2PO_4^-$ on the muscovite surface, which increases the repulsive force between particles and improves the fluidity of pulp. SHMP effectively improves muscovite's grinding efficiency, providing a theoretical basis for the efficient preparation of fine-grained muscovite.

Author Contributions: Conceptualization, C.F. and L.R.; methodology, C.F.; validation, C.F., S.B. and Z.Y.; resources, Y.Z.; writing—original draft preparation, C.F.; supervision, Y.Z.; project administration, L.R.; funding acquisition, L.R. All authors have read and agreed to the published version of the manuscript.

Funding: This research was funded by the National Natural Science Foundation of China (U2003129).

Data Availability Statement: No new data were created or analyzed in this study. Data sharing is not applicable to this article.

Acknowledgments: The authors gratefully acknowledge the National Natural Science Foundation of China (U2003129) for the financial support provided.

Conflicts of Interest: The authors declare no conflict of interest.

References

1. Zhou, Q.; Qin, K.; Tang, D.; Wang, C. A Combined EMPA and LA-ICP-MS Study of Muscovite from Pegmatites in the Chinese Altai, NW China: Implications for Tracing Rare-Element Mineralization Type and Ore-Forming Process. *Minerals* **2022**, *12*, 377. [CrossRef]
2. Chen, G.; Ren, L.; Zhang, Y.; Bao, S. Improvement of fine muscovite flotation through nanobubble pretreatment and its mechanism. *Miner. Eng.* **2022**, *189*, 107868. [CrossRef]
3. Xiao, W.; Peng, Y.; Zheng, S.; Feng, Q.; Zhang, C.; Zhang, J.; Hao, Y.; Liao, M.; Zhou, Y. Thermally Stable and Radiation Hard Ferroelectric $Hf_{0.5}Zr_{0.5}O_2$ Thin Films on Muscovite Mica for Flexible Nonvolatile Memory Applications. *ACS Appl. Electron. Mater.* **2019**, *1*, 919–927. [CrossRef]
4. Chen, J.; Li, S.; Zhong, J.; Wang, B.; Pan, R.; Wang, Z.; Gao, L. The effect of epoxidized natural rubber on mechanical properties of siliceous earth/natural rubber composites. *Polym. Bull.* **2017**, *74*, 3955–3975. [CrossRef]
5. Wang, L.; Li, Z.; Luo, K.; Guan, S.; Ge, W.; Zhang, J. Study on the measurement method for resistivity of mineral powder—Taking micro-crystal muscovite for example. *Powder Technol.* **2011**, *214*, 400–405. [CrossRef]
6. Tohidifar, M.; Taheri-Nassaj, E.; Alizadeh, P. Precursor content assessment and its influence on the optical interference of a nano-sized mica-hematite pearlescent pigment. *Powder Technol.* **2010**, *204*, 194–197. [CrossRef]
7. Shen, F.; Chen, H. The Preparation and Characteristics of a Blue Pearlescent Pigment with LTA-Type Ultramarine Coated on the Mica Substrate. *Nano* **2021**, *16*, 2150065. [CrossRef]
8. Singh, H.; Meghwal, M.; Prabhakar, P.; Kumar, N. Grinding characteristics and energy consumption in cryogenic and ambient grinding of ajwain seeds at varied moisture contents. *Powder Technol.* **2022**, *405*, 117531. [CrossRef]
9. Prziwara, P.; Breitung-Faes, S.; Kwade, A. Comparative study of the grinding aid effects for dry fine grinding of different materials. *Miner. Eng.* **2019**, *144*, 106030. [CrossRef]
10. Mao, Y.; Wang, Z.; Liu, W.; Tian, P. Effect of TIPA/TEA combined grinding aid on the behavior of quartz flotation in DDA system. *Powder Technol.* **2022**, *406*, 117570. [CrossRef]
11. Drahman, S.; Kueh, A.; Zainal Abidin, A.; Nikmatin, S. Efficient cumulative breakage distribution and breakage rate computation with minimal experiment intervention incorporating optimal time determination for fine grinding simulation. *Powder Technol.* **2018**, *329*, 313–322. [CrossRef]
12. Toprak, N.; Benzer, A.; Karahan, C.; Zencirci, E. Effects of grinding aid dosage on circuit performance and cement fineness. *Constr. Build. Mater.* **2020**, *265*, 120707. [CrossRef]
13. Li, H.; Jiang, Z.; Yang, X.; Yu, L.; Zhang, G.; Wu, J.; Liu, X. Sustainable resource opportunity for cane molasses: Use of cane molasses as a grinding aid in the production of Portland cement. *J. Clean. Prod.* **2015**, *93*, 56–64. [CrossRef]
14. Cheng, F.; Feng, Y.; Su, Q.; Wei, D.; Wang, B.; Huang, Y. Practical strategy to produce ultrafine ceramic glaze: Introducing a polycarboxylate grinding aid to the grinding process. *Adv. Powder Technol.* **2019**, *30*, 1655–1663. [CrossRef]
15. Prziwara, P.; Kwade, A. Grinding aids for dry fine grinding processes—Part I: Mechanism of action and lab-scale grinding. *Powder Technol.* **2020**, *375*, 146–160. [CrossRef]
16. Chipakwe, V.; Semsari, P.; Karlkvist, T.; Rosenkranz, J.; Chehreh, C. A critical review on the mechanisms of chemical additives used in grinding and their effects on the downstream processes. *J. Mater. Res. Technol.* **2020**, *9*, 8148–8162. [CrossRef]
17. Yang, J.; Ma, S.; Zhou, W.; Zhu, P. Study on Grinding Additives in Cassiterite–Polymetallic Sulfide Ore Grinding. *Minerals* **2022**, *12*, 472. [CrossRef]
18. Chen, Y.; Lian, X.; Zheng, S. Research on superfine grinding process and kinetics of calcined black talc in planetary mill. *Procedia Eng.* **2015**, *102*, 379–387. [CrossRef]
19. He, Y.; Zhang, X.; Wu, G.; Shi, P. Effects of Polycarboxylate-based Grinding Aid on the Performance of Grinded Cement. *J. Wuhan Univ. Technol. Mater. Sci. Ed.* **2021**, *36*, 682–688. [CrossRef]
20. David, A.; Ali, H.; Timothy, N.H.; John, R.; John, L.E.; Stephen, S.; David, H. Role of sodium hexametaphosphate in ultra-fine grinding of alumina-doped titanium dioxide. *Powder Technol.* **2022**, *397*, 117022.
21. Ren, L.; Zhang, Z.; Zeng, W.; Zhang, Y. Adhesion between nanobubbles and fine cassiterite particles. *Int. J. Min. Sci. Technol.* **2023**, *in press*. [CrossRef]
22. Li, G.; Cai, Y.; Wang, X.; Zhang, L.; Xie, Q.; Chen, P.; Li, C.; Sun, J.; Li, T.; Dong, L. Direct Z-scheme heterojunction rutile-TiO_2/g-C_3N_4 catalyst constructed by solid grinding method for photocatalysis degradation. *Chem. Phys.* **2022**, *559*, 111558. [CrossRef]
23. Bao, S.; Xin, C.; Zhang, Y.; Chen, B.; Ding, W.; Luo, Y. Application of Capacitive Deionization in Water Treatment and Energy Recovery: A Review. *Energies* **2023**, *16*, 1136. [CrossRef]
24. Robinson, T.; Eisenstein, N.; Cox, S.; Stapley, S.; Grover, L. Dispersing heterotopic ossification with hexametaphosphate. *Biomed. Tech.* **2017**, *62*, 167.
25. Rasouli, M.; Abbasi, S.; Azarikia, F.; Ettelaie, R. On the heat stability of whey protein: Effect of sodium hexametaphosphate. *Int. J. Dairy Technol.* **2020**, *73*, 46–56. [CrossRef]
26. Zhang, H.; Zhou, F.; Yu, H.; Liu, M. Double roles of sodium hexametaphosphate in the flotation of dolomite from apatite. *Coll. Surf. A Phys. Eng. Asp.* **2021**, *626*, 127080. [CrossRef]
27. Li, Z.; Han, Y.; Li, Y.J.; Gao, P. Effect of serpentine and sodium hexametaphosphate on ascharite flotation. *Trans. Nonferrous Met. Soc. China* **2017**, *27*, 1841–1848. [CrossRef]

28. Ding, W.; Bao, S.; Zhang, Y.; Xiao, J. Efficient Selective Extraction of Scandium from Red Mud. *Miner. Process. Extr. Metall. Rev.* **2022**. [CrossRef]
29. Sun, L.; Zhang, X.; Tan, W.; Zhu, M.; Liu, R.; Li, C. Rheology of pyrite slurry and its dispersant for the biooxidation process. *Hydrometallurgy* **2010**, *104*, 178–185. [CrossRef]
30. Patcharanat, K.; Douglas, H.; Fumitake, T. Adsorptive reduction of water hardness by a highly porous and regenerative geopolymer fabricated from coal fly ash waste with low-temperature calcination. *Environ. Sci. Pollut. Res. Int.* **2021**, *28*, 54594–54607.
31. Sayin, M.; von Reichenbach, H. Infrared spectra of muscovites as affected by chemical composition, heating and particle size. *Clay Miner.* **1978**, *13*, 241–254. [CrossRef]
32. Wang, Y.; Wen, K.; Dang, W.; Xun, J. Strengthening the inhibition effect of sodium silicate on muscovite by electrochemical modification. *Miner. Eng.* **2020**, *161*, 106731. [CrossRef]
33. Liao, R.; Wen, S.; Liu, J.; Feng, Q. Flotation separation of fine smithsonite from calcite using sodium hexametaphosphate as the depressant in the Na_2S-Pb(II)-KIAX system. *Sep. Purif. Technol.* **2022**, *295*, 121245. [CrossRef]
34. Shishelova, T.; Lipovchenko, E.; Shulga, V. Mica Dehydroxylation Mechanism. *J. Appl. Spectrosc.* **2019**, *86*, 817–821. [CrossRef]
35. Rebolledo, E.; Laskowski, J.; Gutierrez, L.; Castro, S. Use of dispersants in flotation of molybdenite in seawater. *Miner. Eng.* **2017**, *100*, 71–74. [CrossRef]
36. Zhang, Z.; Ren, L.; Zhang, Y. Role of nanobubbles in the flotation of fine rutile particles. *Miner. Eng.* **2021**, *172*, 107140. [CrossRef]
37. Pek-Ing, A.; Siew-Yee, S.; Lavanya, A.; Ee-Meing, L.; Yee-Kwong, L. Muscovite mica and koalin slurries: Yield stress–volume fraction and deflocculation point zeta potential comparison. *Powder Technol.* **2014**, *262*, 124–130.
38. Greta, F. Grinding Media Motion and Collisions in Different Zones of Stirred Media Mills. *Minerals* **2021**, *11*, 185.
39. He, K.; Jia, M.; Sun, F.; Yang, Q.; Wu, B.; Li, X.; Meng, C. Simulation of Grinding Media Motion and Collisions in Wet-Operated Accelerator-Mill Using DEM Coupled with CFD. *Minerals* **2022**, *12*, 341. [CrossRef]
40. Strobel, A.; Schwenger, J.; Wittpahl, S.; Schmidt, J.; Romeis, S.; Peukert, W. Assessing the influence of viscosity and milling bead size on the stressing conditions in a stirred media mill by single particle probes. *Chem. Eng. Res. Des.* **2018**, *136*, 859–869. [CrossRef]

Disclaimer/Publisher's Note: The statements, opinions and data contained in all publications are solely those of the individual author(s) and contributor(s) and not of MDPI and/or the editor(s). MDPI and/or the editor(s) disclaim responsibility for any injury to people or property resulting from any ideas, methods, instructions or products referred to in the content.